NASA Technical Memorandum 88790

NASA-TM-88790 19860021593

Determination of Grain Size Distribution Function Using Two-Dimensional Fourier Transforms of Tone Pulse Encoded Images

Edward R. Generazio
Lewis Research Center
Cleveland, Ohio

June 1986

NASA

ENTER:
SELECT UTP/ANALYSIS *+1 GAS *+
NO HITS SELECTING TERM OR INVALID REFERENCE NUMBER

DISPLAY 41/6/1
86N31065*# ISSUE 22 PAGE 3472 CATEGORY 38 RPT#: NASA-TM-88790
E-3125 NAS 1.15:88790 86/06/00 24 PAGES UNCLASSIFIED DOCUMENT
UTTL: Determination of grain size distribution function using two-dimensional Fourier transforms of tone pulse encoded images
AUTH: A/GENERAZIO, E. R.
CORP: National Aeronautics and Space Administration. Lewis Research Center, Cleveland, Ohio.
SAP: Avail: NTIS HC A02/MF A01
CIO: UNITED STATES
MAJS: /*DISTRIBUTION FUNCTIONS/*FOURIER TRANSFORMATION/*GRAIN SIZE/*IMAGE ANALYSIS/*METALLOGRAPHY/*MICROSTRUCTURE/*SIZE DISTRIBUTION
MINS: / GRAIN BOUNDARIES/ POROSITY
ABA: Author

DETERMINATION OF GRAIN SIZE DISTRIBUTION FUNCTION USING TWO-DIMENSIONAL FOURIER TRANSFORMS OF TONE PULSE ENCODED IMAGES

Edward R. Generazio
National Aeronautics and Space Administration
Lewis Research Center
Cleveland, Ohio 44135

ABSTRACT

Microstructural images may be "tone pulse encoded" and subsequently Fourier transformed to determine the two-dimensional density of frequency components. A theory is developed relating the density of frequency components to the density of length components. The density of length components corresponds directly to the actual grain size distribution function from which the mean grain shape, size, and orientation can be obtained.

E-3125

INTRODUCTION

Material characteristics, such as tensile strength, hardness, yield stress, fracture stress, impact resistance,[1-6] and ultrasonic attenuation[7] are directly related to the grain size distribution in polycrystalline materials. Thus prediction of these properties requires detailed knowledge of the grain size distribution. While the theoretical determination of grain size distribution has received considerable attention.[8] The experimentally measured distribution function has received limited acceptance, primarily due to complexity of real microstructures where the grain topology varies considerably. Hence researchers have acquiesced with determination of the mean or average grain diameter which ideally should be determined from the grain size distribution.

There are currently several accepted techniques[8] for determining the mean grain size without measuring the grain size distribution function. Most methods rely on a line intercepts along random directions or in circular paths;

alternatives estimate the circumference or area of each grain. .Current techniques are not applicable to any arbitrary system and the researcher must often determine which method will yield the most accurate data. The guidelines for making this decision are qualitative generalizations and, as such, can lead to considerable error in the results.[8]

The most common method used for determining mean grain size are the ASTM line intercept and the ASTM comparison method.[8] The line intercept method has been shown to work well for materials having regular grain microstructure; however, this method is not applicable to materials exhibiting oriented or complex, irregular structure, and when applied by different researchers, the line intercept method can lead to results that vary up to 50 percent.[8] The comparison method relies on the researchers judgment in comparing standard ASTM grain charts with the observed microstructure. Neither of these methods is used for determination of the grain size distribution.

This paper describes a technique for determining the grain size distribution function from a metallographically prepared sample. By applying two-dimensional Fourier transform theory to tone pulse encoded microstructural images, the grain size distribution function is determined. The resulting relationship is two-dimensional and yields the grain size distribution, mean grain shape, size and orientation.

THEORY

One Dimensional Fourier Transforms

The Fourier transform of an arbitrary function $f(x)$ is given by.[9]

$$F(u) = \int_{-\infty}^{+\infty} f(x)\, e^{-i(2\pi ux)}\, dx \tag{1}$$

$|F(u)|$ represents a density function such that the number of components contained in the interval $|du|$ is given by[10] $|F(u)||du|$. The variable x may

refer to any quantity such as frequency, time, length, etc. For example, if x is time then u is frequency and $|F(u)|$ represents the density of frequency components. Given a frequency u the period x' is given by $x' = 1/u$. Throughout this work we will refer to x' as the reciprocal variable of u and u as the reciprocal variable of x'.

Equation (1) may be expressed with respect to the period variable,[11] x'.

$$|P(x')||dx'| = |F(u)||du| \tag{2}$$

where $|P(x')||dx'|$ is the number of period components contained in a period interval $|dx'|$. Then

$$|P(x')| = |F(u)| \left|\frac{du}{dx'}\right| \tag{3}$$

using

$$\left|\frac{dx'}{du}\right| = \frac{1}{u^2} \tag{4}$$

we obtain,

$$|P(x')| = |F(u)|u^2 \tag{5}$$

TWO-DIMENSIONAL FOURIER TRANSFORM THEORY

A two-dimensional Fourier transform contains two variables, such as x and y and is given by[9]

$$F(u,v) = \int_{-\infty}^{\infty} \int_{-\infty}^{+\infty} f(x,y)\, e^{-i2\pi(ux+vy)}\, dx\, dy \tag{6}$$

Here the number of components per area interval $|du||dv|$ is given by $|F(u,v)||du||dv|$. Equation (6) may also be expressed in polar coordinates. With $dx\, dy = r d\theta\, dr$ we have[12]

$$F(s,\phi) = \int_{-\pi}^{\pi} \int_{0}^{\infty} f(r,\theta)\, e^{-i2\pi s \cdot r}\, r d\theta\, dr$$

where $s = \sqrt{u^2 + v^2}$ and $r = \sqrt{x^2 + y^2}$

The number of components per area interval is

(8) $$|F(s,\phi)||sd\phi||ds|$$

and the number of components per radial length at an angle ϕ is

(9) $$|F(s,\phi)||ds|.$$

Expressing Equation 9 in terms of period reciprocal variable r' we have

(10) $$|P(r',\phi)||dr'| = |F(s,\phi)||ds|$$

where $|P(r',\phi)|$ is the density of period components in the interval $|dr'|$. Using $s = 1/r'$ we obtain

(11) $$|P(r',\phi)| = |F(s,\phi)|s^2$$

Determination of Boundary Length Distribution Function

Suppose there exists a set of barriers placed along the axis as shown in Figure 1(a). The boundaries are randomly spaced along the x-axis and have the same amplitudes. We are interested in determining the distribution of lengths between the boundaries over the entire length of the x-axis. The Fourier spectra of a three cycle tone pulse having an amplitude 2A, with x' and fundamental frequency $u_o = 3/x'$ is given by

(12) $$|F(u)| = Ax' \left| \left\{ \frac{\sin [\pi(u_o - u)x']}{[\pi(u_o - u)x']} - \frac{\sin[\pi(u_o + u)x']}{[\pi(u_o + u)x']} \right\} \right|$$

If a three cycle, sine wave, tone pulse is formed between adjacent barriers (see Figure 1(b)) the resulting waveform will be made up of a series of tone pulses each having fundamental frequencies at $3/x_i'$, where x_i' refers to the length between the i and $(i + 1)$ barriers. The Fourier transform of the waveform will yield $|F(u)|$, the density of frequency components, and $|P(x')|$ will provide the density of length components (or the length distribution function). Three cycles will correspond to a fundamental period one third the true width between the barriers (This true period or length will

be referred to as the barrier width.). This is easily corrected by rescaling the fundamental periods by a factor of three.

It is possible for the relative phases between the tone pulses to interact by constructive and destructive interference. This would lead to an erroneous density of frequency components where constructive or destructive phase interference dominates. If the phase interference is incoherent (i.e., random) or negligible, then the density of frequency components is accurate.

Here it is assumed that phase interaction between tone pulses is either negligible or incoherent. This is a relatively strong assumption, but it will be shown later to be a reasonable one. It is pointed out that for this work we will use a digital 512 point fast Fourier transform (FFT) which limits the resolution of the x-axis to 512 points.

In order to form a smooth barrier width distribution function 512 random barrier systems similar to that shown in Figure 1(a) will be evaluated. Each of the 512 barrier systems is frequency coded with tone pulses and subsequently Fourier transformed to determine $|F_n(u)|$ where the subscript n refers to the n^{th} barrier system. The total density of frequency components for the entire set of barrier systems is given by

$$|F_t(u)| = \sum_{n=1}^{512} |F_n(u)| \tag{13}$$

from which the total density of length components is obtained

$$|P_t(x')| = |F_t(u)|u^2 \tag{14}$$

Figures 2(a) and (c) show the density of length components and the actual barrier length distribution function, respectively. For lengths less than $x' < 13$ pixels ($u > 0.076$), $|F(u)|u^2$ deviates considerably from the actual barrier distribution function. This deviation originates from the nonnegligible higher order harmonics that are present for a three cycle tone pulse. These high frequency components are enhanced by the factor u^2

(Eq. (14)). Equation (12) indicates that the density of frequency components at the fundamental frequency of a three cycle tone pulse is proportional to the tone pulse width, x'. If the amplitude of each three cycle tone pulse is diminished in proportion to its corresponding width, then the resultant density of frequency components, at the fundamental frequency for each tone pulse, is normalized to a constant value, A. While the higher order harmonics are correspondingly diminished in amplitude. For example, the waveform shown in Figure 1(b) is modified by decreasing the amplitude of each tone pulse by $1/x_i'$ where x_i' is the width of the i^{th} tone pulse. If the phases of the tone pulses exhibit negligible or incoherent interaction then the Fourier transform of the modified waveform for the j^{th} barrier system is

$$|F_j(u)| = \sum_i \left| \mathcal{F}\left[\frac{f_i(x)}{x_i'} \right] \right| \tag{15}$$

where $\mathcal{F}$ denotes the Fourier transform and $f_i(x)$ describes the waveform of the i^{th} tone pulse. Since x_i' is constant for the i^{th} tone pulse we have

$$|F_j(u)| = \sum_i \frac{1}{x_i'} \, |\mathcal{F}(f_i(x))| \tag{16}$$

for the j^{th} barrier system.

The density of frequency components for a set of 512 barrier systems becomes

$$|F_m(u)| = \sum_j |F_j(u)| = \sum_j \sum_i \frac{1}{x_{ij}'} \, |\mathcal{F}(f_{ij}(x))| \approx |F_t(u)|u \tag{17}$$

where the subscript m refers to the modified system. Using Equation (14) the density of length components is

$$|P(x')| = |F_m(u)|u = |F_t(u)|u^2 \tag{18}$$

Equation (18) indicates that when the Fourier spectra of the modified system $|F_m(u)|$ is multiplied by u the density of length components is obtained (compare Equations (18) and (14)). The results follow similarly in two dimensions (from Equation (11)) to yield the density of radial length components at an angle ϕ,

$$|P(r',\phi)| = |F_m(s,\phi)|s = |F_t(s,\phi)|s^2. \tag{19}$$

The approximation in Equation (17) become equivalence when $F(f_i(x))$ approach delta functions[10] at the fundamental frequencies, $u_o = 3/x_i'$. In other words, if the number of cycles in each tone pulse is increased the $|F_m(u)|u$, the density of length components, becomes a more accurate representation of the true density of length components. Unfortunately, increasing the number of cycles of each tone pulse in a digital 512 point array prohibits tone encoding of small lengths. Here, the Nyquist frequency[10] is the limiting factor. Therefore, there is a trade off between the required measurement of small lengths and the required accuracy of the length distribution function.

The resultant modified waveform is shown in Figure 1(c). This modification is done for the entire 512 barrier systems. The density of length components for the modified barrier set is shown in Figure 2(b) and is given by $|P(x')| = |F_m(u)|u$ where one additional factor of u is pre-included in the construction of the modified barrier systems (see Equation (18)). This modification reduces the high frequency enhancement from u^2 to u and yields a more accurate representation of the length distribution function as shown in Figure 2(b). The flat region of the distribution for pixel periods less than 10 pixels is identified as residual noise resulting from higher frequency harmonics. This flat noise region is observed in all systems investigated and is intrinsic in the Fourier transform theory. This easily

identifiable region is clipped to a zero value to eliminate the higher harmonic noise. Figure 2(d) is an overlay of curves shown in Figure 2(a), (b), and (c).

The results shown in Figure 2 indicate that the density of length components corresponds directly to the actual length distribution function. This supports the assumptions that: (1) The phase interaction of tone pulses is incoherent or negligible. (2) The selection of three cycles per length is sufficient to yield an accurate result.

Application of Fourier Transform Theory to Microstructural Images

To apply Fourier transform theory to microstructural images we tone pulse encode the two-dimensional image. The construction of a two-dimensional tone pulse encoded representation of an arbitrary microstructural image requires enhancement of the original image as indicated below. The microstructure of stock nickel 200 is shown in Figure 3(a). The image was digitally recorded into a 512 by 512 pixel array via a vidicon camera connected to a video digitizer. The image is a numerical average of five digitizations. The gray scale resolution of the video digitizer allows for pixel intensities to vary from 0 to 255, where an image intensity of 0 and 255 correspond to black and white, respectively. The grain boundaries are clearly visible as interconnecting dark curves.

The grain boundaries are enhanced by taking the two-dimensional digital gradient[9] (Figure 3(b)) of the microstructure shown in Figure 3(a). A gray level line scan along the x-direction (in Figure 3(b)) at $y = 255$ is shown in Figure 3(c). A series of peaks are observed in this line scan that correspond to the position of the grain boundaries. The peaks vary in amplitude where the magnitude derivative between grains varies in agreement with the optical intensity. Between the peaks there exist noise generated by

variations of the optical intensity within the grains. This noise is also observed in the original microstructural image (Figure 3(a)). The within grain noise is removed by determining the magnitude of the derivative of the weakest (that is, the most difficult to determine optically) grain boundary. All pixels in the gradient image having a value lower than this value are set to zero while all others are set to a constant nonzero value. As a result we have a clean image of the grain structure where each grain boundary is given equal weight (i.e., the same intensity). A gray level line scan along the x-direction at $y = 255$ for the noise reduced, grain boundary enhanced image (Figure 4(a)) is shown in Figure 3(d). The line scan reveals a series of equal amplitude, half cycle pulses. Each pulse corresponds to its respective grain boundary along the scan direction. The enhanced image is a two-dimensional representation of the one-dimensional case shown in Figure 1(a). In order to assure that there is equal weighting of grains in all directions the enhanced image is circularly masked as shown in Figure 4(a). Next a tone pulse encoded image containing the fundamental harmonics of each grain is generated. This is done as in the one-dimensional case. The tone pulse begins at a grain boundary and ends at a grain boundary and has a width equal to the width of the grain. A new tone pulse is started at an adjacent grain boundary which generally has a different width. This is done digitally starting at the center of the image and proceeds outward along a fixed number of radii to the perimeter of the circular mask. The process is repeated for all angles (0 to 2π rad) so that the frequency coded image appears as shown in Figure 4(b). Figure 4(c) is a gray level line scan along the x-direction of Figure 4(b) at $y = 255$ and is similar to that shown for the one-dimensional case (see Figure 1(c)).

Nine different photomicrographs of the same sample are tone pulse encoded and then digitally Fourier transformed using a complex 512 point, hardwired,

fast Fourier transform array processor. The density of length components at an angle ϕ is given by Equation (19) and is shown in Figure 5(a). This figure represents the density of length component as a function of the reciprocal length, s. We may better understand this result by plotting the result in Figure 5(a) as a function of 1/s (i.e., length) as shown in Figure 5(b). Figure 5(b) represents the density of length components as a function of length, r', and corresponds directly to the actual grain size distribution function $|P(r',\phi)|$. From this figure the grain size distribution and mean grain size of the original microstructure may be determined along any direction.

The mean grain length $D(\phi)$ along an arbitrary angle ϕ is obtained from Figure 5(b) and is given as

$$D(\phi) \equiv \frac{\sum_{r'} |P(r',\phi)|\ r'}{\sum_{r'} |P(r',\phi)|} \tag{20}$$

where $r' = \sqrt{x^2+y^2}$

The mean grain shape, size, and orientation obtained from Equation (20) is shown in Figure 5(b) (inset). For this microstructure the mean grain shape is roughly circular with no net orientation.

The grain size distribution along the x-direction ($\phi = 0$), $|P(r',0)|$, is shown in Figure 5(c) as a dark curve. Also shown for comparison is a histogram of the grain size distribution along the x-direction obtained by using a commercially available image analyzer. The histogram exhibits a slight shift in the distribution toward larger grains. This is most probably due to the technique used for determining grain size for this instrument. The histogram obtained is determined by measuring the maximum length (in the x direction) of each grain. Therefore it is expected that the histogram be shifted to toward larger grains. The "tone pulse encoded" and commercial

instrument results yield mean grain diameters (along the x-direction) of 60 and 72 μm, respectively, and differ by 16 percent.

As the mean grain size of a real microstructure is not known a priori and is found to be dependent on the methodology used for its determination[8], it seems appropriate to provide a test system for which the mean grain size, shape and orientation are known. A simulated microstructure containing a distribution of sizes of identically shaped and oriented grains shown in Figure 6(a) was used. After tone pulse encoding, the space between the grains was masked to a zero value tone code to eliminate treating them as "artificial" grains. The resultant density of length components is shown in Figure 6(b). The mean grain size, shape and orientation are obtained by use of Equation (20). The reconstructed mean grain shape and orientation is shown in Figure 6(c) along with the actual mean grain. The reconstructed grain is properly oriented and of similar shape to the actual mean grain. The largest error in the reconstruction of the mean grain has occurred at the regions of sharp radii of curvature (top and bottom of the actual grains). The error at these regions is 12 percent.

This work may also be applied to ceramics for the determination of pore size distribution. Figure 7(a) is a digitally enhanced photomicrograph of a sintered ceramic showing a distribution of pores. The area between the pores was set to a zero value tone code after tone pulse encoding. The pore size distribution function shown in Figure 7(b) exhibits an anisotropic distribution. The mean pore (see Figure 7(b) inset) is oval in shape and is oriented along the vertical axis with an aspect ratio of 10:7.

DISCUSSION

The entire process of digitizing images, image enhancement, tone pulse encoding, Fourier transformation and determination of the grain size

distribution function takes about 15 hr using a nonvirtual minicomputer, hardwired array processor (for FFT) and a video digitizer. The operator needs to interact during the digitization of the microstructural images which takes about 20 min. Most of the computer time is spent reading and writing to the video digitizer. This time could be easily reduced by at least an order of magnitude by using a virtual minicomputer that can perform mathematical operations on an entire image contained in a random access memory array. By comparison the commercial image analyzer requires about 2 hr of operator intensive activity (tracing grain boundaries) to yield grain distribution data along two perpendicular directions.

Since each microstructural image contains a different set of grains the grain size distribution will not be identical for each image. Thus averaging over a number of photomicrographs[10] is necessary to estimate the real grain size distribution. The increase in accuracy of the grain size distribution function is proportional to $\sqrt{N}$ where N is the number of averaged images. Nine images provide for an increase in accuracy by a factor of three; it should be noted that it would take 100 images to increase the accuracy by a factor of 10.

In order to tone pulse encode three full cycles between adjacent boundaries, at lease 10 pixels are required. Therefore, the smallest grain width measurable has a length of 10 pixels, and all grains having widths less than 10 pixels are not included in the determination of the grain size distribution. This is observed in Figure 5(c) where the grain size distribution begins a sharp rise at 10 pixels. The functional form of the grain size distribution is not known for smaller grain widths. It could be argued that more data would be available by tone pulse encoding with one or two cycles instead of three cycles. By using one or two cycles in the tone pulse, grains having widths of 4 or 7 pixels, respectively, could be encoded. In

order to address this argument we must examine the gradient image (Figure 4(a)) where the uncertainty of the grain widths is 3 pixels.

Tone pulse encoding with fewer cycles would allow for the inclusion of smaller width grains (grains having widths 4 to 7 pixels). However, the current uncertainty (3 pixels) in the grain width would remain the same making detailed measurement of these narrow width grains of questionable validity.

The percent uncertainty in the grain width is given by

$|\sigma_x| = \left|\frac{\Delta x}{x}\right| \cdot 100$ percent, where $\Delta x = 3$ pixels and x is the grain width. The percent uncertainty is inversely proportional to the grain width. That is, the larger the grain width to be measured the more accurate the measurement. There is less that 15 percent uncertainty (due to the uncertainty in the grain widths) in the grain size distribution function for grain widths greater than 20 pixels.

This work could be enhanced in several ways. A hardwired tone pulse encoding processor could be used in conjunction with a virtual superminicomputer to reduce the processing speed to a few minutes. Increased accuracy (via averaging) of the distribution function could be available with a computer controlled vidicon camera scanning the actual microstructural surface. Also, an image array greater than 512 by 512 pixels would allow for finer definition of boundaries allowing for tone encoding of narrower widths.

This technique is not limited to grain or porosity distributions. It may also be applied to any system for which the length distribution function is required. Some specific examples are the determination of whisker size distribution function in chopped fiber composites as well as the length distribution function between whiskers. This also applies to continuous fiber composites. In metals the inclusion and metallic phase length distribution functions may be determined. Application of this work to three mutually

perpendicular planar sections will yield the full three-dimensional mean grain and/or pore size, shape, and orientation.

CONCLUSIONS

Microstructural images may be tone pulse encoded and subsequently Fourier transformed in order to determine the two-dimensional density of frequency components. A theory has been developed and applied to relate the density of frequency components to the density of length components. The density of length components corresponds directly to the two-dimensional grain and/or pore size distribution function from which the mean grain or pore size, shape, and orientation are obtained.

REFERENCES

1. Klima, S.J. and Baaklini G.Y., "Nondestructive Characterization of Structural Ceramics," SAMPE Quarterly, Vol. 17, Apr. 1986, pp. 13-19.
2. Evans, A.G., "Aspects of Reliability of Ceramics," Defect Properties and Processing of High-Technology Nonmetallic Materials, Materials Research Society Symposium Proceedings, Vol. 24, J.H. Crawford Jr., Y. Chen, and W.A. Sibley, eds., 1984, pp. 63-80, Elsevier, New York, NY.
3. Petch, N.J., "Cleavage Strength of Polycrystals," Journal of Iron Steel Institute, Vol. 174, May 1953, pp. 25-28.
4. Hall, E.O., "The Deformation and Ageing of Mild Steel: III Discussion of Results," Proceedings Physical Society (London), Vol. 64B, Sept. 1951, pp. 747-753.
5. Dieter, G.E., Mechanical Metallurgy, 1961, McGraw-Hill, New York, NY.
6. Reed-Hill, R.E., Physical Metallurgy Principles, 2nd edition, 1973, Van Nostrand, New York, NY.
7. Generazio, E.R., "Scaling Attenuation Data Characterizes Changes in Material Microstructure," Materials Evaluation, Vol. 44, Feb. 1986 pp. 198-202, 208.

8. DeHoff, R.T., Quantitative Microscopy, 1968, McGraw-Hill, New York, NY.

9. Gonzalez, R.C. and P. Wintz, Digital Image Processing, 1977, Addison-Wesley, Reading, MA.

10. Lynn, P.A., Introduction to the Analysis and Processing of Signals, 2nd edition, 1983, Howard W. Sams & Co., Indianapolis, IN.

11. Blakemoore, J.S., Solid State Physics, 2nd edition, 1974, W.B. Saunders, Philadelphia, PA.

12. Hildebrand F.B., Advanced Calculus for Applications, 2nd edition, 1976, Prentice-Hall, Englewood Cliffs, NJ.

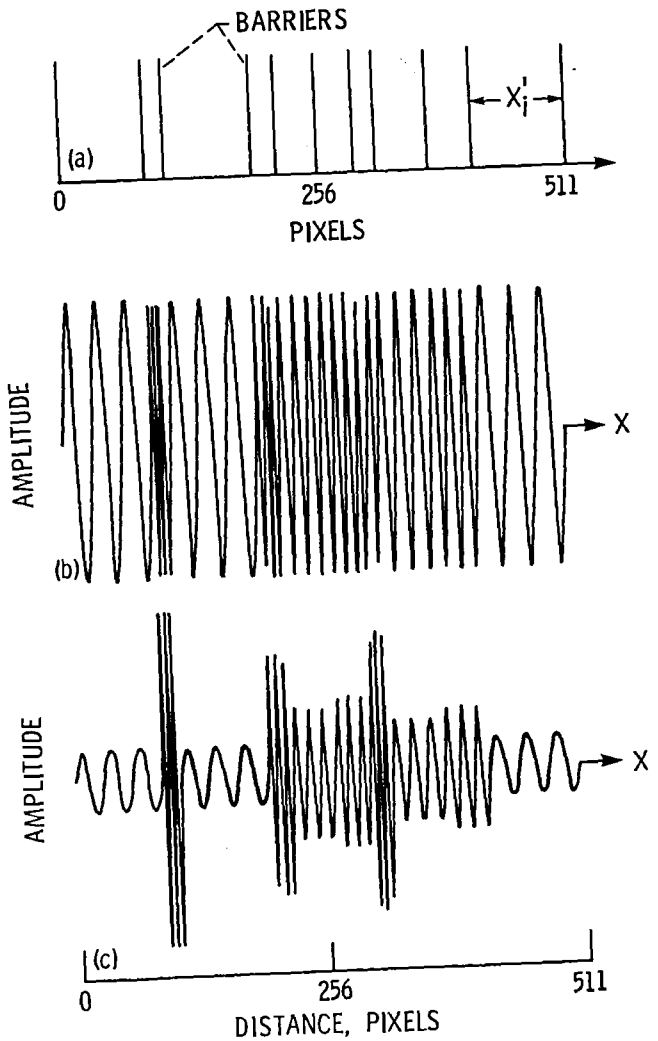
BARRIERS
X_i'
(a)
0
256
511
PIXELS
AMPLITUDE
X
(b)
AMPLITUDE
X
(c)
0
256
511
DISTANCE, PIXELS

FIGURE 1.

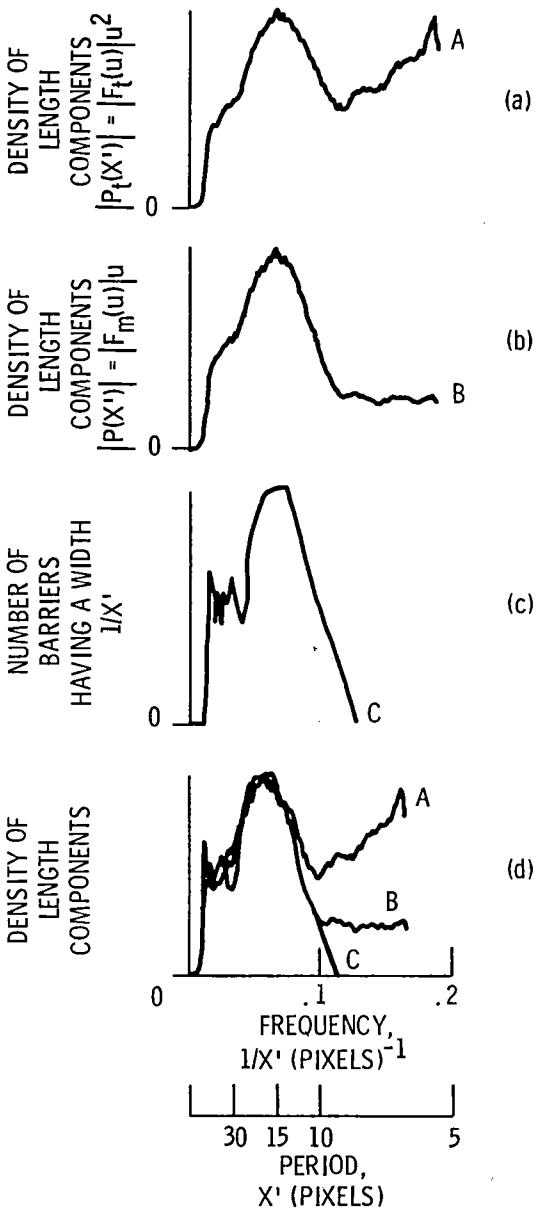
DENSITY OF LENGTH COMPONENTS
$|P_t(X')| = |F_t(u)|u^2$
A
0
(a)
DENSITY OF LENGTH COMPONENTS
$|P(X')| = |F_m(u)|u$
B
0
(b)
NUMBER OF BARRIERS HAVING A WIDTH 1/X'
C
0
(c)
DENSITY OF LENGTH COMPONENTS
A
B
C
0
.1
.2
FREQUENCY, 1/X' (PIXELS)$^{-1}$
30 15 10 5
PERIOD, X' (PIXELS)
(d)

Figure 2.

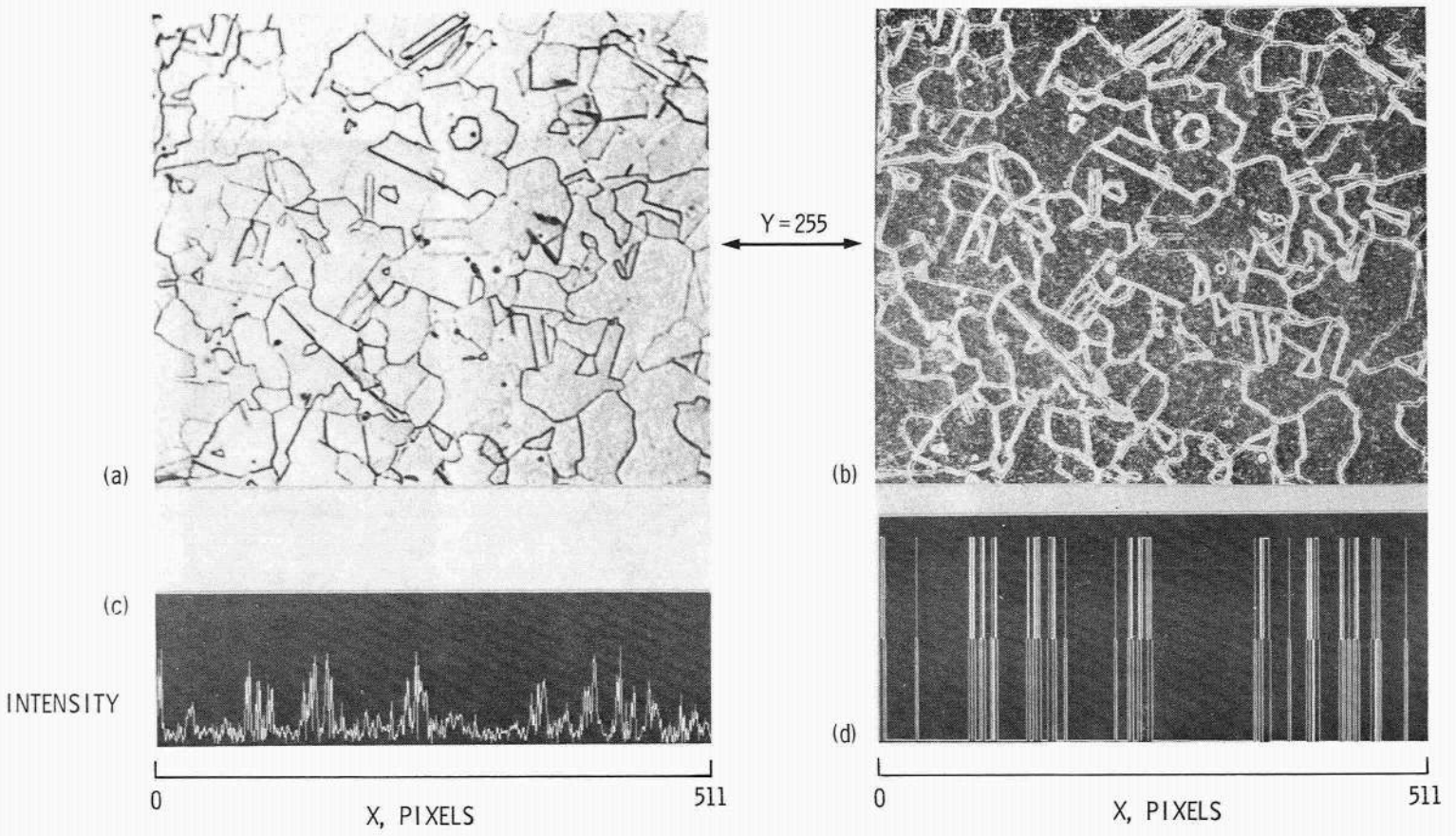

Figure 3.

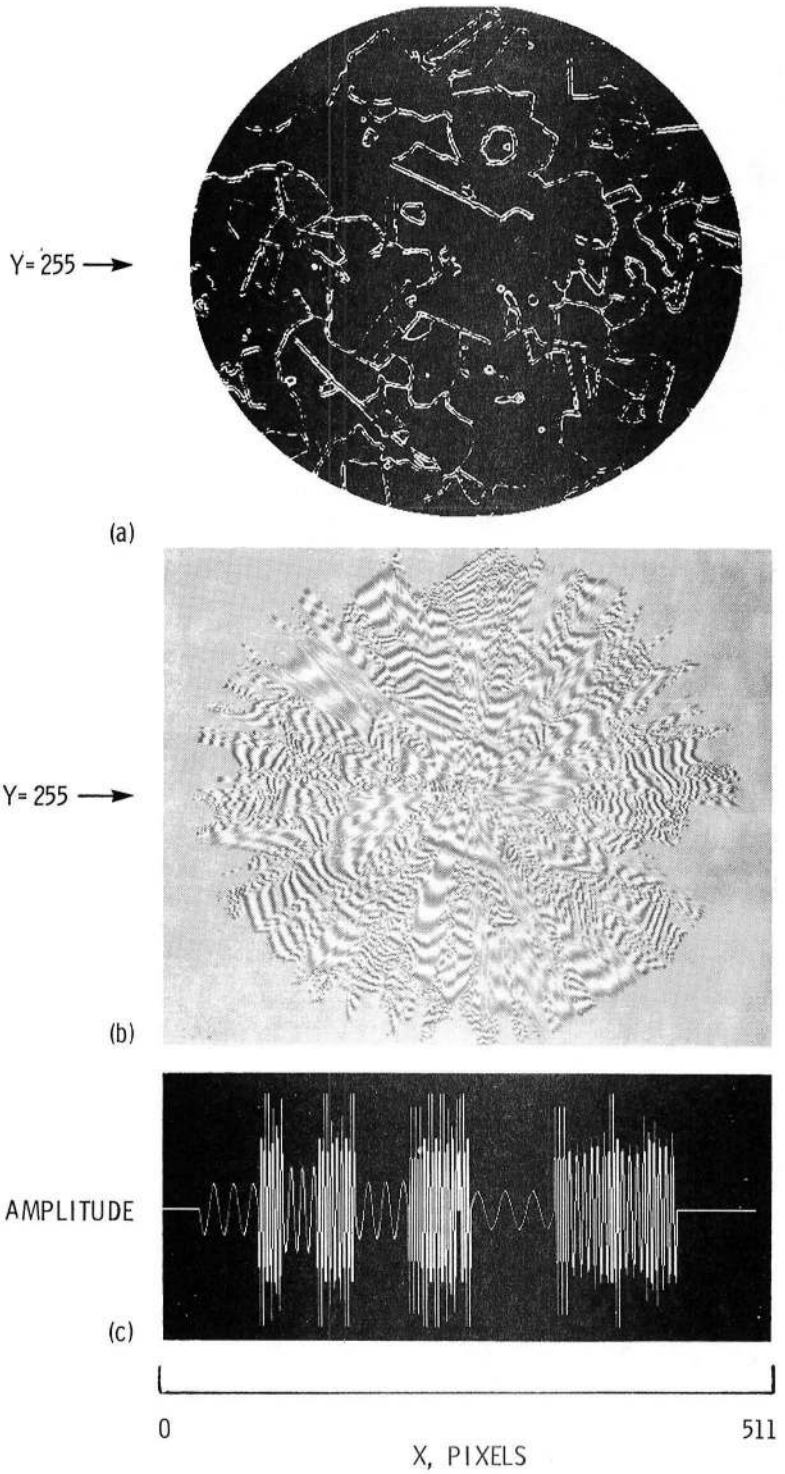

Figure 4.

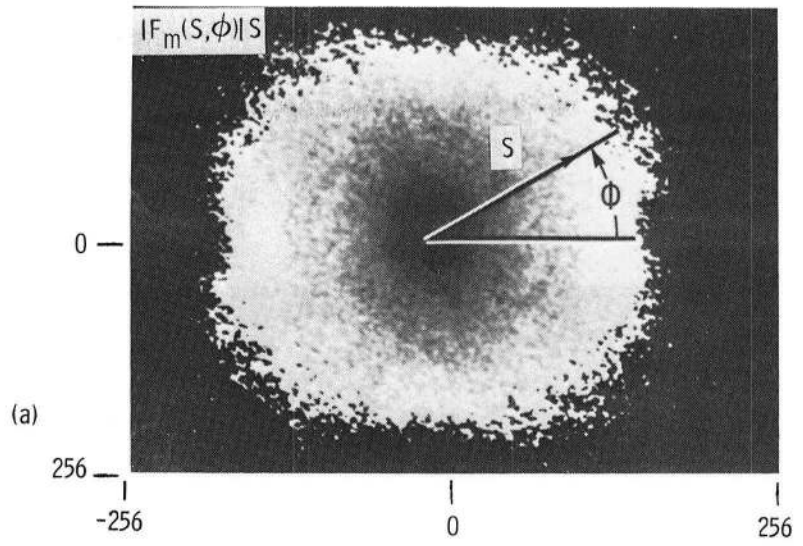
$|F_m(S,\phi)|S$
S
Φ
0
256
-256
0
256

(a)

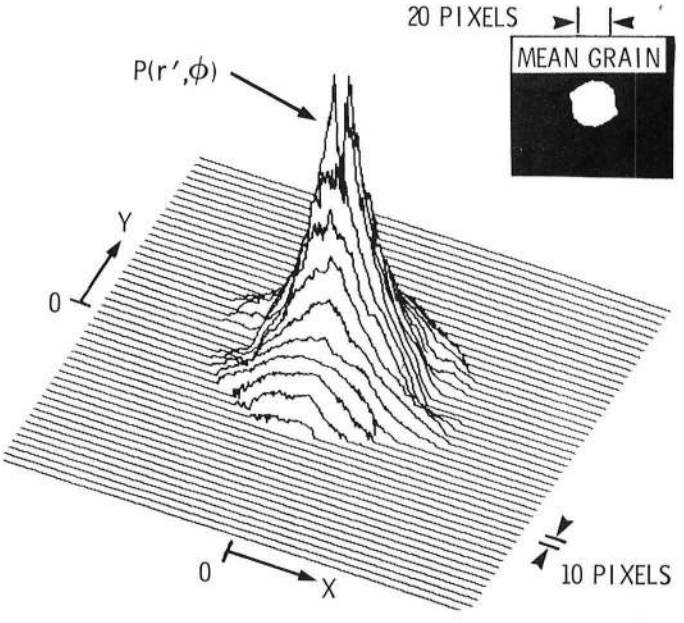
20 PIXELS
MEAN GRAIN
P(r′,ϕ)
Y
0
0
X
10 PIXELS

(b)

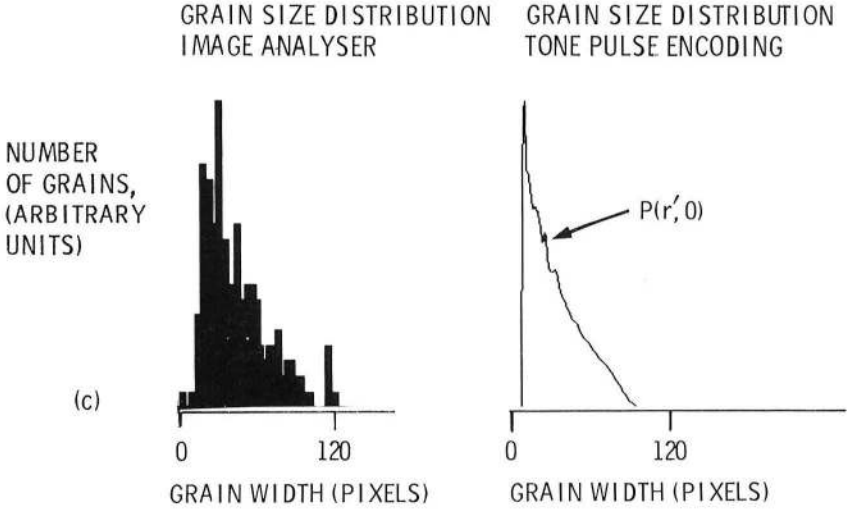
GRAIN SIZE DISTRIBUTION
IMAGE ANALYSER
GRAIN SIZE DISTRIBUTION
TONE PULSE ENCODING
NUMBER
OF GRAINS,
(ARBITRARY
UNITS)
P(r′,0)
0
120
0
120
GRAIN WIDTH (PIXELS)
GRAIN WIDTH (PIXELS)

(c)

Figure 5.

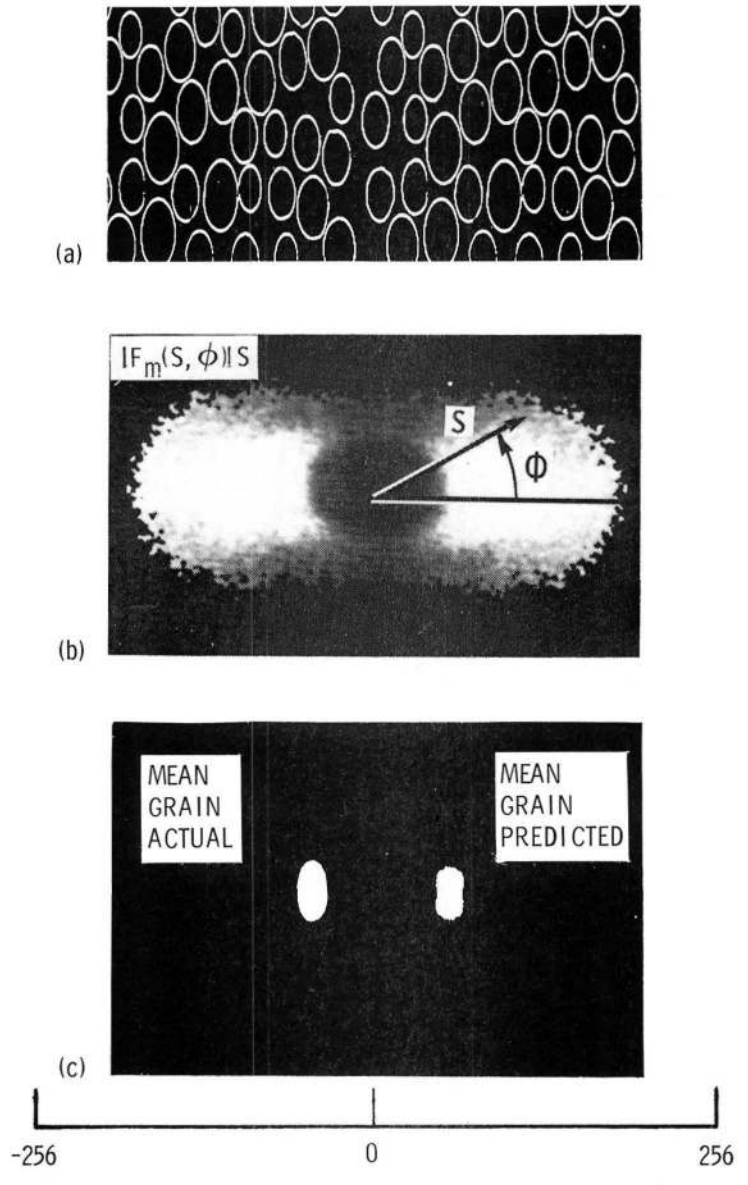
(a)
$|F_m(S, \phi)|$ S
S
Φ
(b)
MEAN
GRAIN
ACTUAL
MEAN
GRAIN
PREDICTED
(c)
-256
0
256

Figure 6.

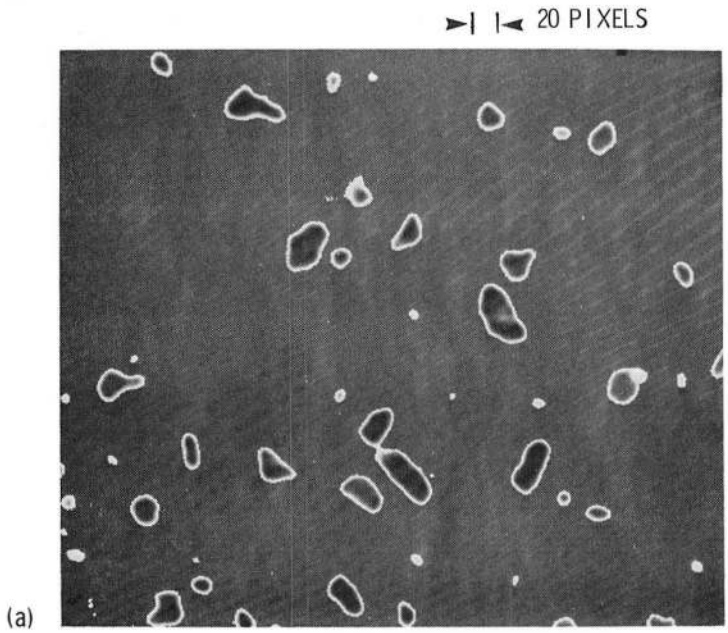

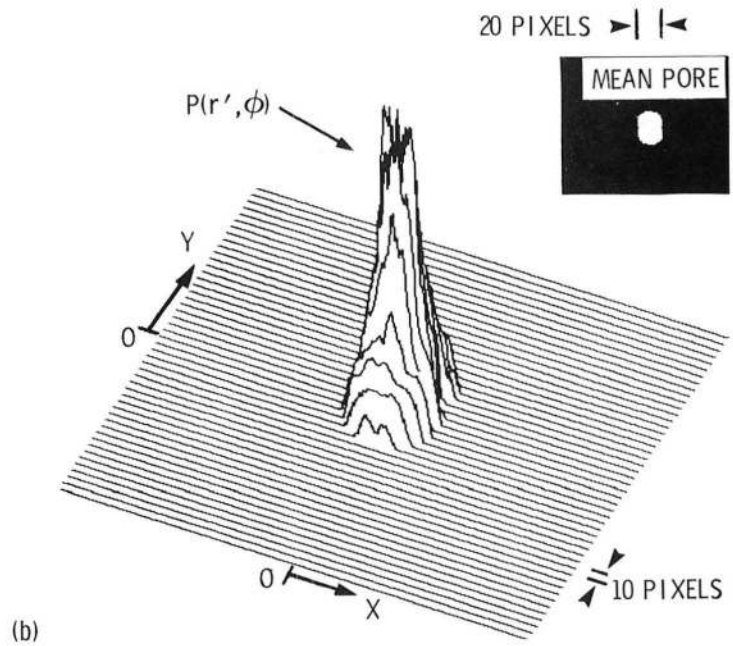

Figure 7.

1. Report No.	2. Government Accession No.	3. Recipient's Catalog No.
NASA TM-88790		

4. Title and Subtitle	5. Report Date
Determination of Grain Size Distribution Function Using Two-Dimensional Fourier Transforms of Tone Pulse Encoded Images	June 1986
	6. Performing Organization Code: 506-43-11
7. Author(s): Edward R. Generazio	8. Performing Organization Report No.: E-3125
	10. Work Unit No.
9. Performing Organization Name and Address: National Aeronautics and Space Administration, Lewis Research Center, Cleveland, Ohio 44135	11. Contract or Grant No.
	13. Type of Report and Period Covered: Technical Memorandum
12. Sponsoring Agency Name and Address: National Aeronautics and Space Administration, Washington, D.C. 20546	14. Sponsoring Agency Code

15. Supplementary Notes

16. Abstract

Microstructural images may be "tone pulse encoded" and subsequently Fourier transformed to determine the two-dimensional density of frequency components. A theory is developed relating the density of frequency components to the density of length components. The density of length components corresponds directly to the actual grain size distribution function from which the mean grain shape, size, and orientation can be obtained.

17. Key Words (Suggested by Author(s))	18. Distribution Statement
Grain size; Distributions; Distribution function; Porosity	Unclassified - unlimited STAR Category 38

19. Security Classif. (of this report)	20. Security Classif. (of this page)	21. No. of pages	22. Price*
Unclassified	Unclassified		

*For sale by the National Technical Information Service, Springfield, Virginia 22161